Thermochimica Acta 510 (2010) 144–153

Contents lists available at ScienceDirect

Thermochimica Acta

journal homepage: www.elsevier.com/locate/tca

Isothermal and non-isothermal crystallization kinetics of ultraviscous melt of $Mg_{65}Cu_{25}Tb_{10}$ glass

D.P.B. Aji, G.P. Johari*

Department of Materials Science and Engineering, McMaster University, Hamilton, ON L8S 4L7, Canada

ARTICLE INFO

Article history:
Received 31 March 2010
Received in revised form 2 July 2010
Accepted 6 July 2010
Available online 13 July 2010

Keywords:
Metal-alloy glass
Crystallization
Isothermal and rate kinetics

ABSTRACT

Crystallization of ultraviscous melt of $Mg_{65}Cu_{25}Tb_{10}$ glass has been studied by two procedures, (i) by keeping the samples at several fixed temperatures, and (ii) by heating the samples at different rates. One prominent exotherm appeared on crystallization in procedure (i), and two appeared on crystallization in procedure (ii). The Kolmogorov–Johnson–Mehl–Avrami relation for the fraction crystallized, $x(t) = 1 - \exp(-kt^m)$, and the corresponding relation for rate-heating, fitted the results from both studies until x began to approach 1 and the measured crystallization rate became slower than the calculated rate. This is attributed to the slower crystallization of inter-granular melt of the same composition as the crystals. The rate coefficient value in $\ln k$ [$\min^{-m}$] increased from −8.25 at 448 K to −1.90 at 468 K with an activation energy of 169 kJ/mol, and m increased from 3.11 to 3.25. On rate-heating at 5 K/min, $\ln k$ [$\min^{-m}$] of the first exothermic peak increased from −21.3 at 458 K to −14.5 at 473 K with an activation energy of 246 kJ/mol and m decreased from 3.30 to 3.20. On annealing the ultraviscous melt, the first peak vanished but the second persisted. On reheating it also vanished. The slower kinetics of the second exothermic peak indicates that the melt crystallized partially to a metastable phase which transformed on heating.

1. Introduction

As a liquid is supercooled, local fluctuation of thermal energy leads to clustering and unclustering of molecules in its bulk. In this stochastic process, clusters that grow to a size larger than the critical size are called nuclei and their number formed per unit time is called the nucleation rate, which increases with decreasing temperature T initially on supercooling, and then decreases on further supercooling. Critical size nuclei grow to form crystals at a rate that depends upon the self-diffusion coefficient in a one-component melt. However, in a multi-component melt, the overall growth rate would be governed by an effective diffusion coefficient that is a combination of partial diffusion coefficients. There are theories for nucleation and crystallization going back to Turnbull and Fisher [1] and the subject has been discussed in detail in two monographs on crystallization and solid–solid transformation, one monograph on crystalline metals and their alloys by Christian [2], and the second monograph on vitreous solids and their melts by Gutzow and Schmelzer [3]. There have been conferences on the subject of nucleation and crystallization of ultraviscous melts [4]. A recent paper [5] has reviewed this subject and provided a scenario for the usual spinodal decomposition and growth of metastable phases in multi-component systems according to the Ostwald's rule of stages.

Depending upon the rate of nucleation and crystal-growth, a glass may contain an insignificant population of nuclei if the nucleation rate near the vitrification temperature on cooling a melt is slow or the glass may contain a large population of nuclei if the crystallization rate is slow. These so-called "athermal nuclei" grow progressively more rapidly as T is increased, thus causing a glass to partially crystallize and thereafter a melt to fully crystallize. In addition, new nuclei form and grow slowly in the same ultraviscous melt. More recently, it has been found that nucleation and crystal-growth also occur in localized regions of a glass structure where diffusive motions of atoms and molecules are faster [6–14]. These localized regions in which thermally activated motions persist in the rigid structure of a glass were known as the β-relaxation [15,16] and are currently known as the JG or the Johari–Goldstein (JG) relaxation [17–19]. In these localized regions in the structure of a glass, as in the regions of dislocations and high defects concentrations in crystalline metals and alloys, nuclei grow to form crystallites. It has been suggested that nucleation and growth in these regions of a glass occur by self-diffusion over a distance shorter than the usual inter-atomic distances. But these regions are not as randomly distributed in the bulk of a liquid as the nucleation sites in the current theories of nucleation and growth. Studies of some ultraviscous melts have shown a so-called induction period for crystallization of some inorganic glasses, an aspect described by

* Corresponding author. Tel.: +1 905 525 9140; fax: +1 905 528 9295.
E-mail address: joharig@mcmaster.ca (G.P. Johari).

0040-6031/$ – see front matter © 2010 Elsevier B.V. All rights reserved.
doi:10.1016/j.tca.2010.07.008

Zeldovich in 1942. Its importance for the understanding of crystallization of melts was first proven by Gutzow and Schmelzer [3] and others [20,21]. Their discussion may be consulted for details. It has been interpreted to indicate the long time required for establishing a steady state distribution of nuclei, the unusually slow growth of the atomic or molecular clusters to a critical size and in some cases to indicate early appearance of metastable phases of the material and its components. When a melt has only one crystal form, the crystal size in the microstructure formed on crystallization may vary depending upon the ratio of the nucleation rate to crystal-growth rate. It has been suggested that even in a one-component melt, the crystal structure of their critical nuclei may also be different from the evolving macroscopic phase and the process may be further complicated by the existence of polymorphism of crystals [5]. But when the crystals formed are compositionally different from the melt, as would occur for non-eutectic compositions (and incongruent freezing/melting), various types of crystals may form on nucleation and crystal-growth. In such a case, microstructure of the solid ultimately formed would vary when the crystal type, size and the melt composition vary in an isothermal nucleation and crystal-growth. In non-isothermal experiments, the temperature-dependence of crystal-growth rate would vary as the composition changes. This would lead to unexpected thermal effects.

During the last decade, production of a number of multi-component metal-alloy glasses in the bulk state by normal cooling of the melt [22,23] has helped establish a discipline of metallic glasses, much like the discipline of polymers, in which basic concepts developed already from studies of nonmetal-alloy glasses are used for interpretation of their glass and crystallization thermodynamics and kinetics. Several reviews on metal-alloy glasses have appeared in recent years [24,25]. Properties of bulk metal-alloy glasses are reasonably stable at ambient temperature as long their glass-liquid temperature range is far above the ambient temperature. Nevertheless, if such glasses are used at high temperatures over a long period of time, or if thermally cycled, not only their structure may continuously relax to that of lower energy, but they may also crystallize to the detriment of their useful properties. A brief review of their structural relaxation thermodynamics has been given in the Introduction of a paper on the calorimetric study of the "memory effect" [26].

Nucleation and crystallization processes in metallic-alloy glasses have certain characteristic of their own, as does their structural relaxation dynamics. Since atoms do not rotate, diffusive motions in their glassy and melts are only translational and there are no internal degrees of freedom or steric hindrance for orientation. In this respect they differ from molecular glasses in which certain orientations are favorable for crystal formation, particularly when such crystals are anisotropic; and they have an entropy of mixing which is in addition to the usual configurational entropy. In the numerous studies on crystallization of metal-alloy glasses since the 1970s, calorimetry has been commonly used as an investigative method [27–30]. Interpretation of such studies has in some cases been supported by using X-ray diffraction and electron microscopy of the samples subjected to a predeterimed thermal history [31–35]. Numerous studies on crystallization of metal-alloy glasses by heating at different rates have been reported. In such experiments the ultraviscous melt crystallizes incongruently whether a glass crystallizes apparently before its glass transition temperature is reached on heating [36–39] or, as in current studies, becomes a relatively stable ultraviscous melt on heating. Analysis of the data obtained from such studies often does not distinguish the various kinetic processes. Moreover, it has been concluded that the assumptions made in analyzing the crystallization kinetics overlook features related to a material's structure, and the parameters obtained by fitting the data to formalisms for crystallization often have little resemblance with the quantities that determine nucleation and crystal-growth [40]. In particular when incongruent crystallization leads to change in the melt composition, the crystal-growth rate changes with temperature as the average inter-diffusion coefficient changes. The change in the diffusion coefficient is taken to be inversely proportional to viscosity of the composition of the melt prior to incongruent crystallization. Calorimetric features of (exothermic) grain growth in nano- and microcrystalline metal alloys [41–43] have also been observed. These features are similar to the features of structural relaxation of metal-alloy glasses [44], and it has been shown that when X-ray diffraction studies cannot distinguish between a glass and a microcrystalline structure, analysis of their calorimetric feature by anneal-and-scan method can be used to determine its glassy state [44].

In view of the above-given features, it is expected that isothermal crystallization studies of metal-alloy glasses would not yield the same results as non-isothermal crystallization studies. Our purpose here is to investigate (i) isothermal crystallization of an ultraviscous melt at several fixed temperatures and (ii) non-isothermal crystallization by heating at several rates and then to determine whether these two experiments yield different results when analyzed by using the current methods. If they do so then the overall kinetics would not appear to be affected by the above-mentioned assumptions and occurrences, and also would not be affected by the usual spinodal decomposition and growth of metastable phases that are known to occur on thermal treatment of inorganic, molecular and polymer glasses, but are either not known in the area of metal-alloy glasses or have not been investigated. Any difference in the total heat of crystallization per mol of the original compositions in isothermal and non-isothermal measurements would reflect the consequences of incongruent crystallization to compositionally different phases.

In addition to showing that calorimetric features of isothermal crystallization kinetics of $Mg_{65}Cu_{25}Tb_{10}$ melt differ from those of non-isothermal crystallization kinetics, and both follow the well-known kinetics of the Kolmogorov–Johnson–Mehl–Avrami equation with similar parameters and yield different activations energies, the study may be useful in extrapolating how a hyperquenched metal-alloy glass of other compositions may partially or fully crystallize in storage or a bulk metal-alloy glass may do so when used as a device at high temperatures. Thermodynamic and kinetics of structural relaxation of the $Mg_{65}Cu_{25}Tb_{10}$ glass were reported in this journal [45]. Our interpretation of the results is necessarily based on calorimetric data. Diffraction and electron microscopic studies that may be used to verify these would ideally require *in situ* high temperature measurements, and these studies are not performed.

2. Experimental methods

The metal-alloy glass samples of composition $Mg_{65}Cu_{25}Tb_{10}$ were prepared by the group of Professor W.H. Wang at Institute of Physics and Center for Condensed Matter Physics, Chinese Academy of Sciences, Beijing, China, and its 0.5 g samples were kindly donated to us by Dr. P. Wen for our study. The procedure they had used was, (i) arc melting of an accurately weighed mixture of pure elements under a titanium-gettered argon atmosphere and (ii) transferring the melt to a water-cooled copper crucible inside which it vitrified also done in argon atmosphere to prevent any oxidation. The melt was homogenized by raising the temperature of the glassy solid far above T_g two to four times. Plate-like specimens of thickness 1–3 mm, width 5–10 mm, and length of 30–40 mm and rod specimens of diameter 3–5 mm and length of 30–40 mm were produced.

A Pyris Diamond PerkinElmer DSC was used with argon as purge gas for the sample holder. The instrument was calibrated with

indium and zinc by using their melting points and their enthalpy of melting. During the course of measurements on a sample, the baseline, temperature calibration and stability of the equipment was frequently checked. An accurately weighed, nominally 7–15 mg, amount of the sample was placed in an aluminum-pan and crimp-sealed. It was transferred to the instrument at ambient temperature. Repeat measurements showed that the DSC output in Watts ($J\,s^{-1}$) divided by the sample's mass remained constant to within 0.2%. Thus the effect of the sample's mass on the measured values was negligible.

Crystallization kinetics was studied, (i) in isothermal mode by keeping the sample at a fixed temperature T_{cryst}, and measuring with time the heat released in $W\,g^{-1}$, and (ii) in scanning modes by heating the sample at a fixed rate and measuring the heat released in $W\,g^{-1}$ with increasing T. Before performing the isothermal crystallization, the usual DSC heating scan was obtained for a heating rate of 20 K/min. This yielded the glass softening temperature T_g of 414 K, and a specific heat increase of 13.3 J/(mol K) in the T_g range, the temperature for onset of crystallization, T_x, and the temperature of the exothermic minimum in the heat flow rate on crystallization. This minimum is here referred to as exothermic peak, T_p, which appeared in this experiment at 483.2 K. For isothermal studies of crystallization, the features of this DSC scan were used for choosing T_{cryst} such that crystallization rate at T_{cryst} would be slow enough to allow measurement of the heat flow with a reasonably accuracy by DSC. This temperature was less than T_p.

For each isothermal study of crystallization, a new sample of the as-cast glass was heated from 363 K at 100 K/min rate to the above-mentioned selected temperatures, T_{cryst}, of 448 K, 453 K, 458 K, 463 K, and 468 K and kept at that temperature for a predetermined time period. After crystallization appeared to have been completed, the sample was cooled to 363 K and thereafter reheated at 20 K/min to a temperature slightly higher than T_x in order to determine if further crystallization or other thermally detectable transformation may occur. None of the samples showed an exothermic minimum on this reheating. Their featureless DSC scans are not shown here.

For each non-isothermal study, the as-cast sample was heated at a fixed rate from 363 K to a certain temperature, T_{max}, and its DSC scan was obtained. The heating rates for this study were 5 K/min, 10 K/min, 20 K/min, 40 K/min and 80 K/min. During the first heating, the characteristic crystallization feature appeared as the exothermic minimum in dH/dt against T plot, which is referred to as T_p. The sample was then cooled to 363 K at the same rate as the heating, and then rescanned to the same T_{max} of 693 K in order to determine whether or not the sample had fully crystallized.

To investigate whether non-isothermal crystallization produced the same calorimetric state as isothermal crystallization, DSC rescans of the crystallized samples from the two studies were obtained and compared. The two DSC rescans were found to be identical within experimental errors. They did not show the glass transition and/or crystallization minimum.

3. Results and data analysis

The plots of dH/dt against the time, t, are shown in Fig. 1, where the chosen temperature at which the sample was isothermally kept for crystallization, T_{cryst}, is noted. In all cases, this temperature is higher than T_g of 414 K for $Mg_{65}Cu_{25}Tb_{10}$ glass for heating at 20 K/min rate. The plots show only one exothermic peak, which is due to overall crystallization of the melt. As expected for a thermally activated process, increasing the sample's T_{cryst} shifts the minimum to a higher temperature, increases its height, makes it narrower and sharper, and reduces the time taken for full crystallization. However, a distinct feature appears in the plot obtained at the lowest

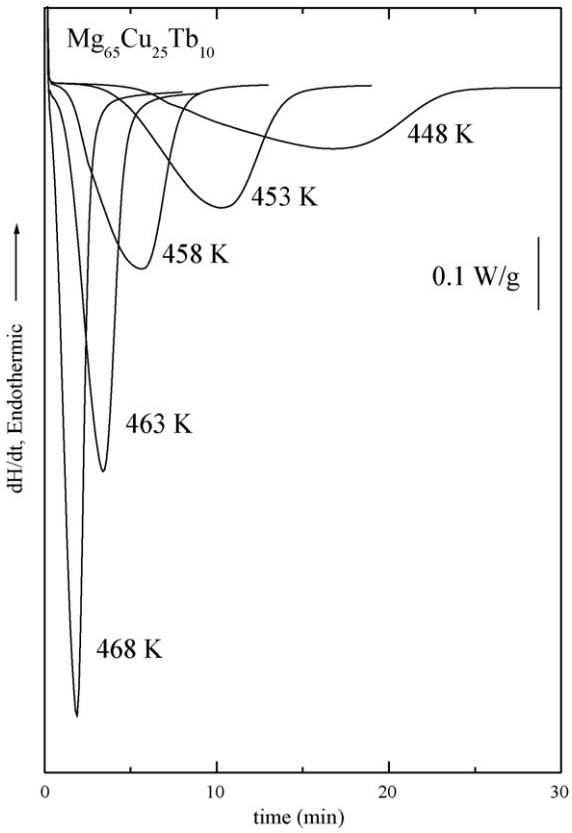

Fig. 1. The plots of dH/dt against time of the ultraviscous melt during isothermal crystallization at 448 K, 453 K, 458 K, 463 K, and 468 K.

temperature of 448 K. Here, the broad peak appears to have become distorted near the beginning.

The plots of dH/dt against T were obtained for heating at a rate, q_h of 5 K/min, 10 K/min, 20 K/min, 40 K/min and 80 K/min. These are shown in Fig. 2. There are two exothermic peaks at temperatures $T_{p,1}$ and $T_{p,2}$ as the $Mg_{65}Cu_{25}Tb_{10}$ glass gradually crystallizes. The onset temperatures of the peaks are labelled as $T_{x,1}$ and $T_{x,2}$. The low-temperature peak is much more prominent than the high temperature peak. This indicates that there are two crystallization processes occurring at different rates. As is expected, when q_h is increased, $T_{p,1}$ and $T_{p,2}$ and $T_{x,1}$ and $T_{x,2}$ increase and the height of the peaks increases.

The partial area of the peak in Fig. 1 is proportional to x, the volume fraction of the sample crystallized at time, t, at the relevant temperature,

$$x(t) = \frac{1}{\Delta H_{cryst}} \int_{t=0}^{t} \left(\frac{dH}{dt}\right) dt \quad (1)$$

where ΔH_{cryst} is equal to the total peak area of the crystallization exotherm. The values of ΔH_{cryst} obtained from isothermal crystallization of $Mg_{65}Cu_{25}Tb_{10}$ melt are listed in Table 1 and those from non-isothermal experiments are listed in Table 2. At the initial time

Table 1
The fixed temperature of crystallization, the enthalpy of crystallization, and the KJMA parameters of crystallization kinetics of $Mg_{65}Cu_{25}Tb_{10}$ ultraviscous melt.

T_{cryst} (K)	ΔH_{cryst} (kJ/mol)	k (min^{-m})	m	E (kJ/mol)
448	2.81	2.6×10^{-4}	3.11	
453	2.92	1.7×10^{-3}	3.15	
458	2.96	5.5×10^{-3}	3.17	169
463	3.23	0.026	3.21	
468	3.61	0.15	3.25	

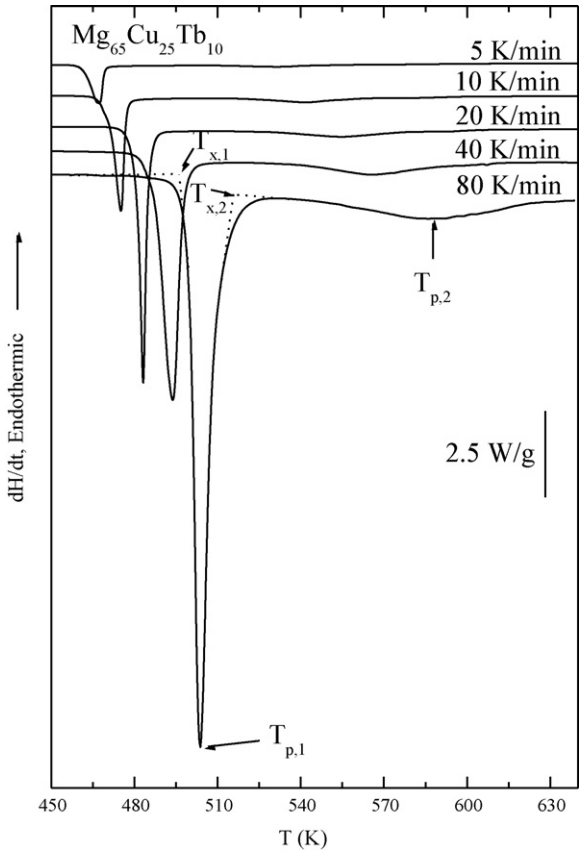

Fig. 2. The plots of dH/dt against T of the glass during heating at rates of 5 K/min, 10 K/min, 20 K/min, 40 K/min, and 80 K/min. $T_{x,1}$ and $T_{x,2}$ are the onset crystallization temperatures for peak 1 and peak 2, respectively. $T_{p,1}$ and $T_{p,2}$ are the peak temperatures for peak 1 and peak 2, respectively.

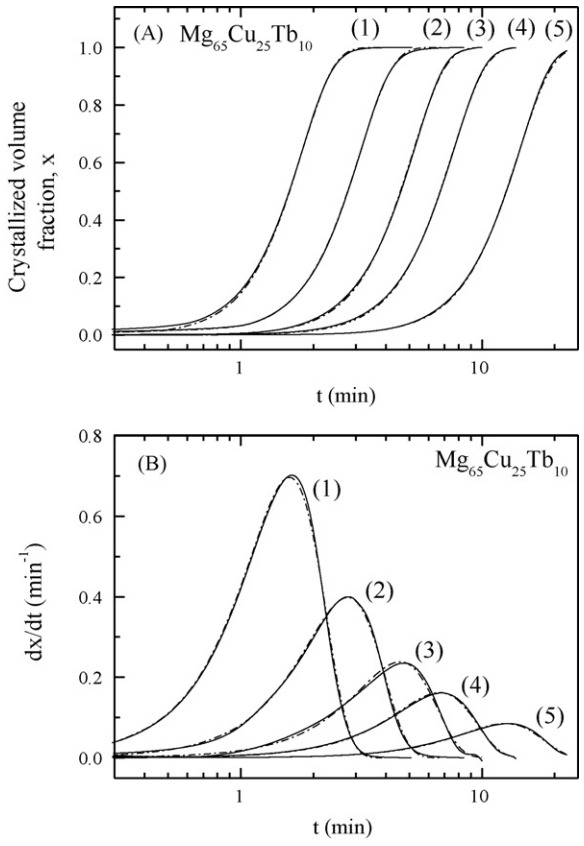

Fig. 3. (A) The crystallized volume fraction plotted against time and the fitting of the KJMA equation to data at, (1) 468 K, (2) 463 K, (3) 458 K, (4) 453 K, and (5) 448 K. (B) The corresponding rate of crystallization. Solid lines are the experiment data and the dash lines are the fitting curves.

which is taken as zero, $x = 0$ and at time near the end of the experiment, $x = 1$. The quantity x was calculated from the data in Fig. 1 and is plotted against t in Fig. 3A. The corresponding plots of the rate of crystallization, dx/dt, are shown in Fig. 3B. Since this rate, is proportional to $-$dH/dt, the dx/dt plots would be equivalent to the inverted plots of Fig. 1.

Similarly, the plots in Fig. 2 were used to obtain x at different temperatures from the relation,

$$x(T) = \frac{1}{\Delta H_{cryst}} \int_{T'}^{T} \frac{1}{q_h} \left(\frac{\mathrm{d}H}{\mathrm{d}t}\right) \mathrm{d}T \qquad (2)$$

where ΔH_{cryst} here is equal to the total peak area in the plot of (dH/dt)/q_h in the temperature plane, and T' is a reference temperature below $T_{x,1}$ or $T_{x,2}$. The rate of crystallization is then obtained from, dx/d$t = q_h$ (dx/dT). The quantities x and dx/dt obtained for peak 1 are plotted against T in Fig. 4A and B, and the corresponding quantities for peak 2 are plotted against T in Fig. 5A and B.

4. General features and formalisms for isothermal and non-isothermal crystallization

It appears that the general concepts and analysis that had been developed for congruent crystallization of (mono-component or eutectic composition) glasses and melts have been used for crystallization of multi-component non-eutectic compositions. In as much as these concepts are used for interpreting the data for metal-alloy glasses, it seems worth mentioning their theoretical and experimental context, and their limitations: according to Turnbull and Fisher's theory of crystal-growth [1–5,46], the rate of homogeneous nucleation is determined by two quantities, (i) the extent of supercooling denoted by $(T_m - T)$, where T_m is the equilibrium freezing point of the melt, and (ii) the excess entropy of supercooled melt over the crystal phase. Kinetic equations for the nucleation rate require also the solid–melt interfacial energy and the free energy barrier for molecular diffusion across the interface, and this barrier may change with both t and T when crystal formed do not have the same composition as the melt. As the melt is cooled, the term

Table 2
The heating rate, the onset and peak temperatures, the enthalpy of crystallization, and the KJMA parameters of crystallization kinetics on rate-heating the $Mg_{65}Cu_{25}Tb_{10}$ glass for the first exothermic feature. Also listed are the onset and peak temperatures, and the enthalpy of crystallization for the second exothermic feature. The fitting method used is similar with the one used by Greer [62].

q_h (K/min)	$T_{x,1}$ (K)	$T_{p,1}$ (K)	$\Delta H_{cryst,1}$ (kJ/mol)	ln k_0	m	E (kJ/mol)	$T_{x,2}$ (K)	$T_{p,2}$ (K)	$\Delta H_{cryst,2}$ (kJ/mol)
5	461.9	466.9	3.47	191.90	3.30		469.5	530.7	0.76
10	469.8	475.2	3.51	190.10	3.28		477.5	541.6	0.85
20	478.2	483.2	3.58	187.01	3.26	246	487.1	553.5	0.89
40	484.3	493.9	3.74	183.25	3.23		498.8	565.9	0.97
80	496.1	503.8	4.05	180.30	3.20		515.7	585.9	0.99

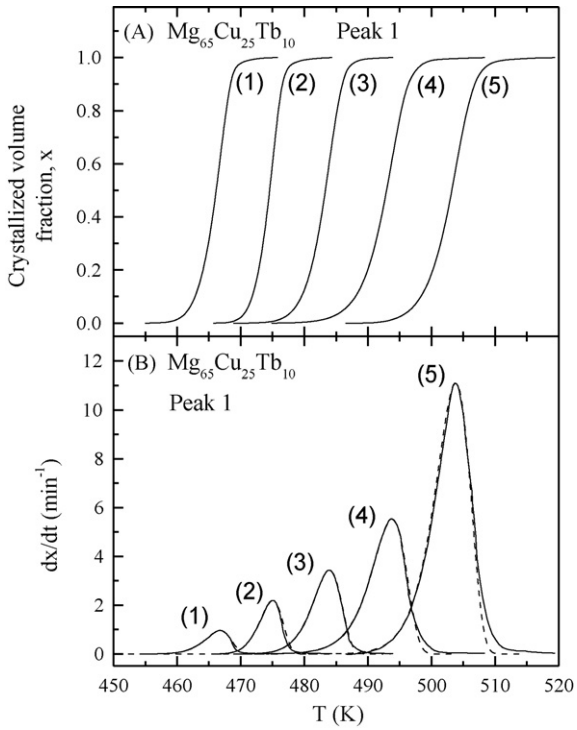

Fig. 4. (A) The crystallized volume fraction from peak 1 is plotted against the temperature. The data were obtained for heating at, (1) 5 K/min, (2) 10 K/min, (3) 20 K/min, (4) 40 K/min, and (5) 80 K/min. (B) The corresponding plots of the crystallization rate plotted against temperature. Solid lines are the experiment data and the dash lines are the fitting curves.

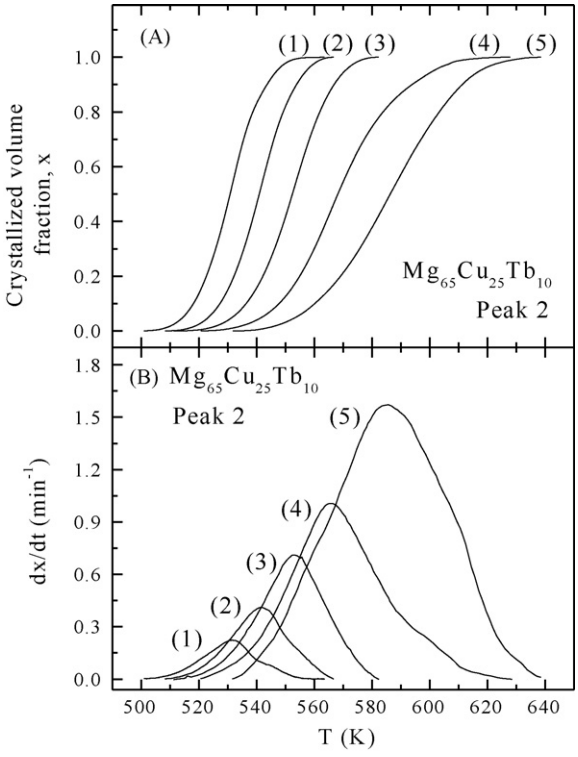

Fig. 5. (A) The crystallized volume fraction from peak 2 is plotted against the temperature. The data were obtained for heating at, (1) 5 K/min, (2) 10 K/min, (3) 20 K/min, (4) 40 K/min, and (5) 80 K/min. (B) The corresponding plots of the crystallization rate plotted against temperature.

$(T_m - T)^2$, that appears in the denominator of the negative exponential term for the nucleation rate (see Refs. [2–5,20,21]), increases rapidly and hence the nucleation rate increases from a low to a high value over a small temperature range. The assumption of constant excess entropy with increasing supercooling restricts the use of the Turnbull–Fisher equation to a small extent of supercooling. For deep supercooling to T far below T_m, the excess entropy becomes significantly less than that at T_m. This lessening not only has a significant effect on the nucleation rate, but also on the crystal-growth rate if the excess entropy were to determine the viscosity, as in thermodynamic theories of glass formation [47]. (Multi-component glasses also have entropy of mixing that does not change on cooling.) In the terminology of thermodynamic and kinetic driving forces for crystallization, (i) the effect of increase in $(T_m - T)^2$ is relatively small at T just below T_m and large in the ultraviscous melt, particularly on cooling toward the vitrification range and (ii) the effect of reduction in the excess entropy is large at T just below T_m and small in the ultraviscous melt on cooling toward the vitrification range. Nucleation rate is zero at T_m and crystal-growth rate is vanishingly small in the vitrified state. Plots of both the nucleation and crystal-growth rates against T show a peak. Their widths and shapes differ and the plots often partly overlap. Recent reviews on this subject have provided details of these effects [4,5,46].

The above-mentioned separation between the time scales of nucleation and crystal-growth, recognized already by Tammann [48] as two consecutive stages of crystallization, is now used for developing the time–temperature profiles for producing glass ceramics of different microstructures and properties by both homogeneous and heterogeneous nucleation [49,50]. Plots of the nucleation and crystal-growth rates against T also have different shapes, and when an ultraviscous melt obtained by heating a glassy state crystallizes, the crystal nuclei, if already present, are expected to grow before new nuclei may form preferably in the localized regions in the glassy state or else form randomly in the volume of an ultraviscous melt. Both the nucleation and crystal-growth rates determine the crystallization kinetics of the melt but the slower of the two rates dominates the observed thermal effects. In contrast, crystallization of metal-alloy glasses by Ichitsubo et al. [12–14], by use of radio-frequency ultrasonic energy absorption has shown that mechanical instability due to the resulting shear in local regions, where the faster process of JG relaxation occurs [51], causes crystallization. Also, as nucleation and crystal-growth occur in the same volume of a melt, the amount of melt available for nucleation decreases as crystals grow. The situation becomes further complicated for incongruent crystallization, because in this case the composition and properties of the remaining melt also change.

Molecular diffusion dynamics that is needed for crystallization of an ultraviscous melt and glass is distinguished from that of a low-viscosity melt. In the ultraviscous melt, it is said to be co-operative and is described in terms of either the characteristic time for the α-relaxation process or viscosity, both of which show a non-Arrhenius variation with T. Their apparent activation energies decrease as T is increased. There is also a dynamics of localized motions that shows up as the β- or the JG relaxation, and whose characteristic time varies with T according to the Arrhenius equation. In the glassy state, the co-operative dynamics is too slow and only the JG relaxation dynamics is observed and yet heat treatment of metal-alloy glass changes its shear modulus [52]. Localized modes of motions are also recognized as the source of the unexpectedly rapid nucleation and growth in the glassy and ultraviscous states of small molecule organic substances [6–11], and there are indications that the overall crystallization rate is most rapid in a viscous melt far below its freezing point [53], at the Donth temperature [54], where the α-relaxation process evolves from the JG relaxation process [51,55].

Kolmogorov [56] had calculated the probability of nucleation in a certain volume that remains available at a certain time after crystallization has begun. Gutzow and Schmelzer [3] have provided a detailed discussion of the subject and compared the Kolmogorov's probability calculation with Poisson's probability calculation of a mathematically similar problem. They also discussed the formal treatments of the volume available for nucleation in a partially crystallized melt by Johnson and Mehl [57] and by Avrami [58,59]. Their description [3], which seems relevant to metal-alloy glasses, may be consulted for details. More recent experiments [6–14] showing that nucleation and crystal-growth occurs in local regions imply that these processes are not necessarily as random as is implicit in the Poisson distribution. It has not been possible to incorporate it in the kinetics of nucleation and crystal-growth, and the incongruent crystallization of metal-alloy glasses makes it more difficult to mathematically interpret crystallization kinetics. As we are unable to take these aspects into account, we analyze our data, as in numerous earlier studies of phase transformation in crystalline metals, and crystallization of molecular and polymeric and metal-alloy glasses, by using the Kolmogorov–Johnson–Mehl–Avrami (KJMA) equation [56–59] for overall crystallization. Accordingly, the quantity x is written as,

$$x_n(t) = 1 - \exp[-Y_n(t)], \quad \text{and} \quad Y_n(t) = \omega_n J v^n \int_0^t (t - t')^n \mathrm{d}t' \qquad (3)$$

where Y_n is the new phase formed until time t, J is the nucleation rate, v is the linear growth velocity and ω_n is a geometrical factor equal to $4\pi/3$ for spheres. The parameter n has different values for different nucleation and growth mechanisms and for dimensions of space in which transformation occurs. These values have been listed in Table 10.1 in Ref. [3]. After substitution for the integral for $Y_n(t)$, the final equation is now known as Kolmogorov–Johnson–Mehl–Avrami (KJMA) equation. Burbelko et al. [60] have reviewed its progress since Kolmogorov's original paper. We follow the description in the monograph by Gutzow and Schmelzer [3]:

$$x_n(t) = 1 - \exp\left[-\frac{\omega_n}{n+1} J v^n t^{n+1}\right] \qquad (4)$$

or

$$x_n(t) = 1 - \exp[-k_n t^{n+1}], \quad \text{where} \quad k_n = \frac{\omega_n}{n+1} J v^n \qquad (5)$$

The quantity $n+1$ is written as equal to m, which is known as the KJMA coefficient for phase transformation. The quantity k_n is known as KJMA kinetic coefficient. Macroscopically, it is the temperature-dependent rate constant for crystallization in this study. The value of m is usually an integer, which depends upon the dimensionality and morphology of the crystal-growth.

In the formalism for nucleation and crystal-growth in molten metals, interactions between atoms have a spherical symmetry, i.e., there is no directional bias, and in molecular melts interactions are also taken to be spherical but in terms of the van der Waals forces. Any change in these interactions may be seen as a process occurring concurrently to crystal-growth, and this change is expected to show up as decrease in the enthalpy. This aspect is also discussed in Ref. [3]. The form of KJMA equation used for fitting the overall, isothermal crystallization kinetics data is:

$$x(t) = 1 - \exp[-kt^m]; \qquad \frac{\mathrm{d}x}{\mathrm{d}t} = mkt^{m-1} \exp(-kt^m) \qquad (6)$$

(Note that Eq. (6) is also written as $x(t) = 1 - \exp[-(kt)^m]$ which simplifies subsequent calculations, as discussed in detail by Bruijn et al. [61]).

5. Discussion

5.1. Thermodynamic aspects

In Table 1, ΔH_{cryst} of $Mg_{65}Cu_{25}Tb_{10}$ melt increases from 2.81 kJ/mol from T_{cryst} of 448 K to 3.61 kJ/mol for T_{cryst} of 468 K. In Table 2, (H_{cryst} for peak 1 increases from 3.47 kJ/mol for q_h of 5 K/min to 4.05 kJ/mol for q_h of 80 K/min and the peak itself shifts from 466.9 K to 503.8 K. Also, (H_{cryst} for peak 2 increases from 0.76 kJ/mol for q_h of 5 K/min to 0.99 kJ/mol for q_h of 80 K/min and the peak shifts from 530.7 K to 585.9 K. If crystallization occurred congruently and there were no other thermodynamic occurrences, the (H_{cryst} values would be closely similar for the five temperatures listed in Table 1. Also, the total (H_{cryst} value for peaks 1 and 2 would be similar for the five heating rates. Moreover, the (H_{cryst} value determined from isothermal crystallization would be similar to that determined from non-isothermal crystallization. Any difference in the total heat of crystallization per mol of the original compositions ($Mg_{65}Cu_{25}Tb_{10}$) in isothermal and non-isothermal measurements would be a consequence of incongruent crystallization to compositionally different phases. The differences observed here indicate that crystallization is incongruent and the calculations based on per mol of the original composition of $Mg_{65}Cu_{25}Tb_{10}$ are not directly comparable. This behavior also has been observed in Fe-based metal-alloy glass [36].

5.2. Features of isothermal and non-isothermal crystallization

In Fig. 3A and B, we have fitted Eq. (6) to the plots of x against t and the values of m and k thus obtained for isothermal crystallization at five temperatures are listed in Table 1. The k values in turn were used to determine the rate constant k_0 and the activation energy E from the relation,

$$k = k_0 \exp\left(-\frac{E}{RT}\right) \qquad (7)$$

When the nucleation rate is negligibly small over the temperature range of interest, E is identified as the activation energy for crystal-growth. The data for $\ln(k)$ obtained from isothermal crystallization studies are plotted against $1/T$ in Fig. 6.

The parameters for the crystallization kinetics on rate-heating were obtained also by fitting the KJMA equation modified for the purpose. It is worth noting that there are several such modifications used for performing such an analysis, but one suggested by Greer [62] seems most appropriate for our use. Greer assumed that the crystallization at different T would vary only in the time scale, i.e., that the transformation is iso-kinetic and its rate at any instant depends only on T and x at that instant. It is independent of prior thermal history of the sample, as would be the case for a melt in which only one type of crystals of only one composition form. In this study, direct use is made of the isothermal KJMA equation by approximating the linear heating profile as a series of short isothermal anneals. Consider a material transformed at T_1 for a time of t_1. The transformed fraction at T_1 is $x = f_1(t')$, where t' is the time from the start of the transformation at T_1. At the end of transformation at T_1, the transformed fraction is $x = f_1(t_1)$. The transformation continues at T_2 for a time of t_2 at which $x = f_2(t'')$, where t'' is the time from the start of transformation at T_2. The course of the transformation at T_2 is precisely the same as if the initial transformed fraction at T_2, $f_1(t_1)$, had been formed at T_2. If $t_{1'}$ is the time it would have taken at T_2 to produce $x = f_1(t_1)$, i.e., $f_1(t_1) = f_2(t_{1'})$, the transformation at T_2 is given by,

$$x = f_2(t + t_{1'} - t_1) \qquad (8)$$

where t is the time from the start of the transformation at T_1 (or T_2). At the end of transformation at T_2, $x = f_2(t_2 + t_{1'} - t_1)$. The calculations were performed by using a computer algorithm in which

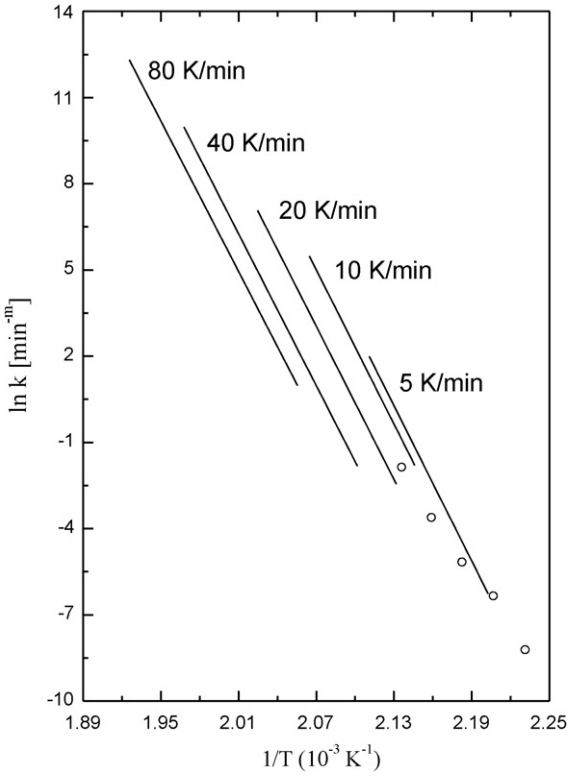

Fig. 6. The plots of ln(k) against the reciprocal temperature. Circles are data from isothermal kinetics, and lines from the rate-heating kinetics.

the temperature was uniformly incremented. At the end of the rate-heating, the value of x was obtained and dx/dt evaluated at the midpoints of temperature step. For the ith increment, dx/dt at $T=(T_i+T_{i+1})/2$ was taken to be $(x_{i+1}-x_i)/(t_{i+1}-t_i)$. Fig. 4B shows the result of fitting of the dx/dt plots for crystallization peak 1 at different heating rates. The fitted parameters for the crystallization kinetics are listed in Table 2. The ln(k) value obtained by this fitting is plotted against $1/T$ in Fig. 6, and the E value is listed in Table 2. (Yinnon and Uhlmann [63] have critically reviewed the eight mathematical methods for fitting the KJMA equation to the non-isothermal crystallization kinetics data, including the widely used Kissinger's [64] method. For reasons given by them [63], we did not use any of these methods for analyzing our data for non-isothermal crystallization kinetics [65].)

The activation energies obtained by the two methods differ: for isothermal crystallization, $E=169$ kJ/mol in Table 1 and for non-isothermal crystallization $E=246$ kJ/mol in Table 2. Although both values are considerably high they are less than those observed for molecular ultraviscous melts, e.g., E for isothermal crystallization for syndiotactic polystyrene is 792 kJ/mol [66]. It is also worth noting that E of $Pd_{77}Cu_6Si_{17}$ and $Pd_{48}Ni_{32}P_{20}$ glasses [67] were determined by non-isothermal crystallization studies, and it was found to be equal to the activation energy for viscous flow, decreasing with increase in the crystallization temperature range on increase in the heating rate. The equality led to the conclusion that crystallization rate is controlled by viscosity. In another study, it was suggested that crystallization in the amorphous solid [68] may occur by a diffusion-less mechanism, in which case E is low and hence the crystallization rate is slow. This is reminiscent of crystallization occurring as a result of localized motions of the JG relaxation, as mentioned here earlier. However, it is now considered that generally speaking crystallization is instead diffusion-controlled.

One of our finding is that the overall crystallization occurred in one thermal step in isothermal experiments, and in two thermal steps in non-isothermal experiments. It is to be noted that multiple peaks in non-isothermal experiments have been observed before in other metal-alloy glasses [30,69–73]. We also observe a small further broadening to the left (shorter times) of the already broad peak, but only for isothermal crystallization at 448 K in Fig. 1. As this feature appears before the main crystallization exotherm it would corresponds to a faster kinetics. Therefore, we expect that a correspondingly small feature from this faster process would appear at the low-temperature side of the first peak in the non-isothermal experiment. But no such feature was observed in Fig. 2. As isothermal crystallization at 468 K is complete in less than 10 min according to the plot in Fig. 1, and 468 K is considerably below 510-580 K range at which $T_{p,2}$ appears in Fig. 2, we may estimate the temperature $T_{p,2}$ at which the second peak might appear at zero heating rate, i.e., isothermally, by extrapolation. This temperature is 525 K.

The exponent, m, is interpreted such as to determine the manner in which nuclei grow to form crystals. Its magnitude is seen to indicate the mechanism of crystal-growth [2,3]. For isothermal crystallization, the value of m listed in Table 1 varies from 3.11 to 3.25. For non-isothermal crystallization at different heating rates m listed in Table 2 is in the 3.2–3.3 range. According to the criteria for crystal-growth [2,3], both sets of m values would suggest that crystallization occurs by interface-controlled growth with decreasing nucleation rate. Since our study is focused on thermal effects of crystallization, we did not confirm the validity of these interpretations by X-ray diffraction and electron microscopy studies.

5.3. Deviations from KJMA equation and crystallization kinetics

It is understood the KJMA equation is at best an adequate fitting equation for overall thermal effects and it cannot be related to a molecular phenomenon, but since such deviations have often been neglected we briefly consider these here. The plots in Fig. 3 show that in the beginning of isothermal crystallization at 468 K, the measured x deviates from the best fit of the KJMA equation. There are also deviations in the plots of the rate of crystallization, but the deviations are small and negligible in view of the measurements and analysis errors. The plots in Fig. 4 show that for non-isothermal crystallization at different heating rates both x and the crystallization rate (dx/dt) deviate considerably from the best fit of the KJMA equation. The deviation seems to be highest at high temperatures where the measured values are more spread out than the calculated values. The calculated values also show, as expected for a thermally activated process, a relatively sharp decrease. It should be noted that in comparison with the deviations from the KJMA equation observed for other metal-alloy glasses in several earlier studies [62,74,75], deviations from the KJMA equation observed for $Mg_{65}Cu_{25}Tb_{10}$ are much smaller and seem negligible in this study.

To investigate the source of this deviation, we determined the ratio of the measured rate of crystallization to that calculated, for both isothermal and non-isothermal crystallizations. This ratio is plotted in Fig. 7A and B, respectively. For isothermal crystallization, the plots in Fig. 7A show a positive deviation by at most 25% at short times when crystallization occurs at 468 K. For higher temperatures, the deviation is less. This may be partly due to the errors in the fitting as well as in experiments and these errors are more pronounced in dx/dt than in the value of x.

For non-isothermal crystallization, the maximum deviation of the plots of measured $(\mathrm{d}x/\mathrm{d}T)_q$ against T in Fig. 7B is much greater, reaching a factor of 1.4 relative to calculated values at the highest temperatures. In the absence of any effects that may increase the heat evolution and thus add to $-\mathrm{d}H/\mathrm{d}t$, this would indicate that crystallization of the melt becomes faster than expected from the

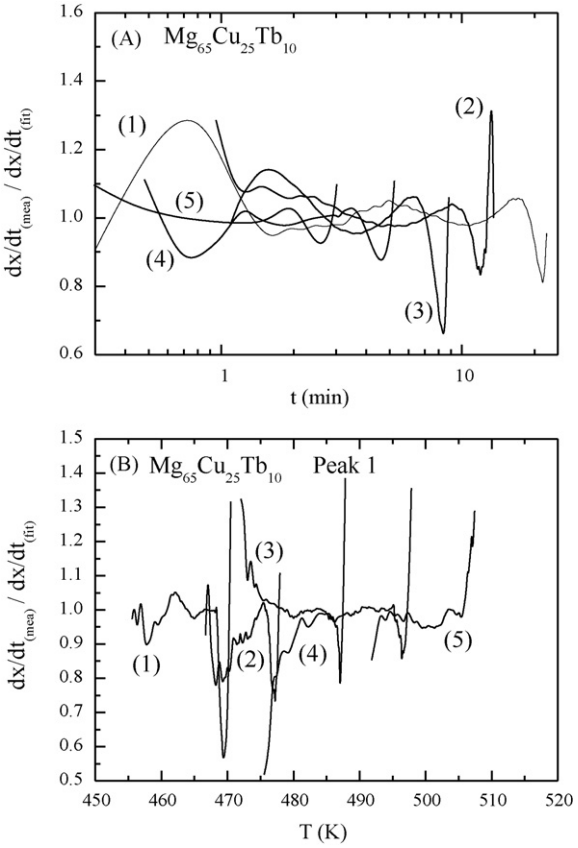

Fig. 7. (A) The ratio of the measured rate of crystallization to that calculated from fitting the KJMA equation is plotted against time. The data are taken from Fig. 3B. (B) The corresponding plots against the temperature from data in Fig. 4B.

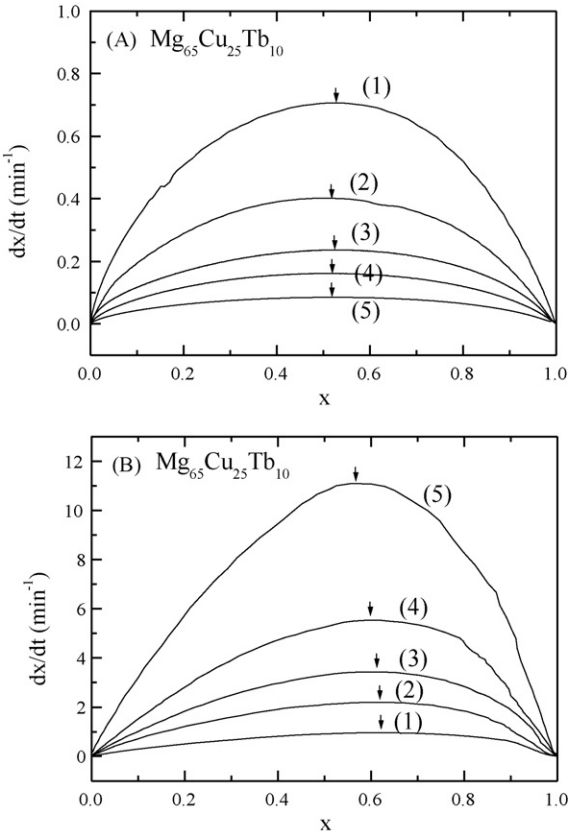

Fig. 8. (A) The rate of crystallization is plotted against the extent of crystallization at, (1) 468 K, (2) 463 K, (3) 458 K, (4) 453 K, and (5) 448 K. (B) The corresponding plots from the data obtained for heating at, (1) 5 K/min, (2) 10 K/min, (3) 20 K/min, (4) 40 K/min, and (5) 80 K/min.

KJMA equation as $x \to 1$. Alternatively, it may indicate additional heat evolution if (i) micron-size crystal grains formed initially grew rapidly as T increased, (ii) some or all of the inter-granular melt crystallized more slowly than the bulk, (iii) the melt composition changed on incongruent crystallization and it slowed the crystallization process more when $x \to 1$, and (iv) the crystals formed underwent a solid–solid transformation.

We also investigate how the rates of isothermal and of non-isothermal crystallization change with the extent of crystallization. Fig. 8A shows the plots of $(dx/dt)_T$ against x isothermally and Fig. 8B shows the corresponding plots for heating at different rates. According to Eq. (6), a plot of $(dx/dt)_T$ against t would show a peak only when $m > 1$, which of course is roughly evident from the sigmoid-shaped plots of x against t in Fig. 3A. The plots of $(dx/dt)_T$ against x in Fig. 8A shows a hump-like feature whose peak shifts from $x = 0.52$ at 448 K to $x = 0.53$ at 468 K, as indicated by the arrows. The relatively small shift is mainly due to change in m with the crystallization temperature. In contrast a broad peak is observed in Fig. 8B, and this peak shifts from $x = 0.62$ at 5 K/min to $x = 0.56$ at 80 K/min, as indicated by the arrows.

5.4. Origin of the second peak on non-isothermal crystallization

In Fig. 2A and Table 2, the high temperature and low-intensity exothermic peak shifts to higher temperatures as the heating rate q_h is increased. In contrast, the first peak shifts much more. This indicates irreversible occurrence of an additional process in the ultraviscous melt or in the crystal formed in the first crystallization. If such a second exotherm were observed for a one-component melt, it would indicate, (i) grain growth in some of the fine structure or nanocrystalline phases formed as a result of the first crystallization, or (ii) a solid–solid transformation to a more stable crystalline phase. These processes may also occur here. But they seem unlikely for a ternary melt of $Mg_{65}Cu_{25}Tb_{10}$ unless its crystals melted and froze congruently. It is also conceivable that the melt initially crystallized non-congruently to form an inter-metallic compound, leaving behind a melt rich in one component. If nucleation and growth in this latter melt were slow, its crystallization would produce a broad exothermic peak at higher temperatures. In physical terms, it is conceivable that the two peaks are a consequence of the difference in the locations of the maxima for nucleation and crystal-growth in a melt that begins to crystallize non-congruently.

The enthalpy decrease associated with the second exotherm (appearing as peak 2) is 0.89 kJ/mol for heating rate of 20 K/min. The enthalpy released in the first crystallization peak is 3.58 kJ/mol for heating rate of 20 K/min as in Table 2, and for the isothermal crystallization is 2.81–3.61 kJ/mol, as given in Table 1. This is only ~78–85% of the enthalpy released in the first peak observed in Fig. 2, and it seems to be a substantial thermal effect. But we point out that such comparisons may be misleading because when incongruent crystallization occurs, the original composition of $Mg_{65}Cu_{25}Tb_{10}$ can not be used for determining the per mole amount of ΔH_{cryst} for either the first peak or the second peak. Also, in a case where the surface of compositionally different crystals acts as a heterogeneous nucleation site, crystallization of the remaining melt would be faster than that observed from homogeneous nucleation and its rate would vary with the amount of crystals present and distribution of the crystal size. This is not observed in the data for $Mg_{65}Cu_{25}Tb_{10}$ here. For that reason we may use the KJMA equation also for the second exothermic peak, but its broadness makes it difficult to separate it satisfactorily from the low-temperature peak.

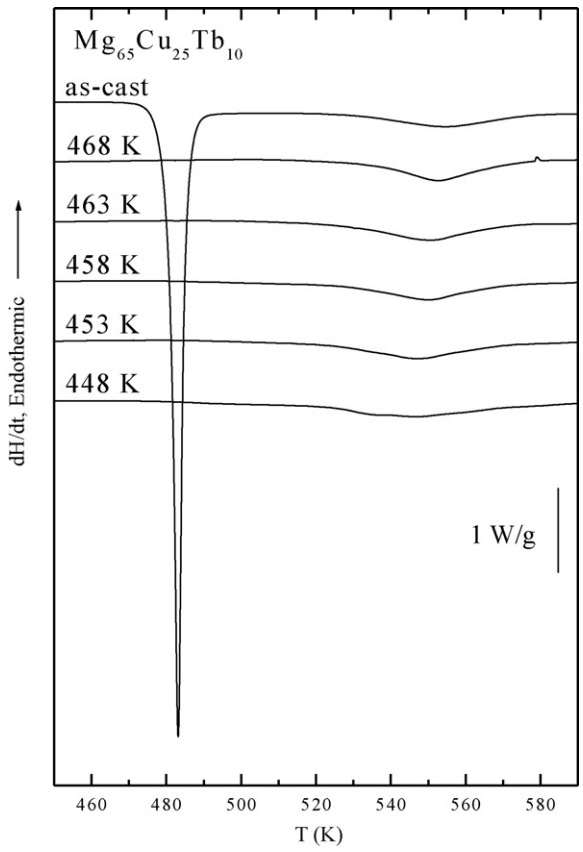

Fig. 9. The plots of dH/dt against T of ultravisocus melt during heating at 20 K/min of the as-cast sample of $Mg_{65}Cu_{25}Tb_{10}$ glass without annealing and after isothermal annealing of its melt at 448 K for 40 min, at 453 K for 25 min, at 458 K for 20 min, at 463 K for 15 min, and at 468 K for 10 min.

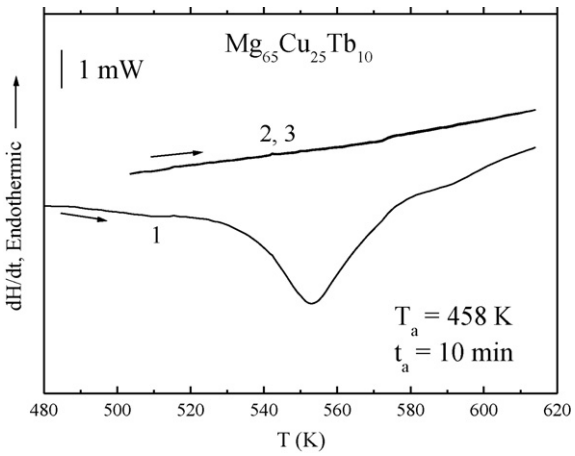

Fig. 10. The plots of dH/dt against T of the glass that was annealed at 458 K for 10 min then heated at 20 K/min, as shown by curve 1. The scan did not show the first peak but the second peak persisted. The curves 2 and 3 were obtained by reheating the sample to 613 K. These showed no features.

To investigate the origin of the second exothermic peak in Fig. 2, we performed a further experiment by annealing the melt. A new sample of $Mg_{65}Cu_{25}Tb_{10}$ glass was heated at 20 K/min from 300 K to 458 K (~44 K above the T_g of 414 K) and then kept isothermally at 458 K for 20 min. Thereafter, the sample was heated from 458 K to 613 K at a rate of 20 K/min. The plot obtained is shown as curve labeled 458 K in Fig. 9. The experiment was repeated for annealing of new samples at 448 K for 40 min, at 453 K for 25 min, at 463 K for 15 min and at 468 K for 10 min periods. These plots are included in Fig. 9, where the plot obtained on heating the sample without annealing is included. The data show that the first crystallization peak vanishes and the second peak is broader after annealing at 448 K and becomes narrower after annealing at 468 K.

In a further experiment, $Mg_{65}Cu_{25}Tb_{10}$ glass was heated to 458 K (~44 K above the T_g of 414 K) and then kept isothermally at 458 K for 10 min. Thereafter, the sample was reheated from 458 K to 613 K at a rate of 20 K/min. The curve obtained is shown as curve 1 in Fig. 10. It shows no features until a temperature of 480 K is reached and thereafter an exotherm appears as in Fig. 9. This shows that annealing of the ultraviscous melt at 458 K for 10 min does not remove the second exothermic peak. Since annealing was done at ~44 K above its T_g, it is unlikely that a significant amount of melt would have persisted after 10 min. (When compared against the plot at 458 K in Fig. 1, this annealing condition amounts to extending the isothermal experiment for 10 more minutes at 458 K.) The sample was then cooled back to 495 K at 20 K/min and reheated at the same rate, and curves 2 and 3 in Fig. 10 were obtained. These show no indication of a further exotherm. The enthalpy released on this reheating is 1.40 kJ/mol (of the $Mg_{65}Cu_{25}Tb_{10}$ composition) in comparison with 0.89 kJ/mol given in Table 2 for the same heating rate without annealing. Vanishing of the exotherm may indicate that crystallites growing at different sites produced a solid containing extremely small grains and hence a large surface area, and annealing was insufficient for grain growth to reach completion. But the 1.40 kJ/mol of the heat evolved for $Mg_{65}Cu_{25}Tb_{10}$ composition from curve 1, seems too large for surface energy reduction by grain growth of particles. It is possible that a metastable phase had formed on annealing and it transformed to a stable phase on heating a process for which the heat evolved would seem acceptable. But we also realize that $Mg_{65}Cu_{25}Tb_{10}$ may not be a ternary eutectic composition in which case crystallization would be incongruent, leaving behind a melt that crystallizes at a slower rate. It seems that the latter occurrence is more probable.

6. Conclusion

Isothermal crystallization of the $Mg_{65}Cu_{25}Tb_{10}$ ultraviscous melts at several fixed temperatures shows only one exothermic feature. This is in contrast with the non-isothermal crystallization at several heating rates that shows two exothermic features over a shorter total time. The total heat evolved on isothermal crystallization of $Mg_{65}Cu_{25}Tb_{10}$ melt varies with the crystallization temperature and that evolved on non-isothermal crystallization varies with the heating rate. The heat of crystallization in the isothermal experiment is less than the total heat of crystallization in non-isothermal experiment. The second exotherm is exceptionally broad when the heating rate is high. This shows that the $Mg_{65}Cu_{25}Tb_{10}$ melt crystallizes incongruently and the heat of crystallization per mole may not be determined by using the $Mg_{65}Cu_{25}Tb_{10}$ composition. The remaining melt of a different composition has a higher viscosity and or slower overall rate of crystallization. There also may be exothermic effects of grain growth but the enthalpy change seems too large for its occurrence. Isothermal crystallization at different temperatures shows no such occurrence.

Crystallization of ultraviscous melts is interpreted in terms of classical nucleation and growth kinetics and the KJMA equation for one-component liquid with temperature-dependent exponent m. Its magnitude indicates that both isothermal and non-isothermal crystallizations are predominantly interface-controlled. The activation energy determined from isothermal crystallization kinetics is ~69% of the activation energy determined from the rate-heating kinetics.

As crystallization approaches completion, the fraction crystallized isothermally at the lowest temperature is slightly more than that calculated from the KJMA equation, and the rate of crystallization shows random deviation, but the rate of non-isothermal crystallization in the first step is slightly higher at high temperatures for the high heating rate. The broad and small second exothermic peak observed in non-isothermal experiments is likely to be due to slower crystallization of the melt that persists after incongruent crystallization of a melt or a solid–solid transformation.

Acknowledgments

This study is part of the Ph. D. thesis of D.P.B. Aji. It was supported by a Discovery Grant from NSERC to GPJ.

References

[1] D. Turnbull, J.C. Fisher, J. Chem. Phys. 17 (1949) 71.
[2] J.W. Christian, The Theory of Transformations in Metals and Alloys, 2nd ed., Pergamon Press, Oxford, 1975.
[3] I. Gutzow, J. Schmelzer, The Vitreous State: Thermodynamics, Structure, Rheology and Crystallization, Springer, Heidelberg, 1995 (Chapter 10).
[4] See articles in: J.W.P. Schmelzer (Ed.), Nucleation Theory and Applications, Wiley–VCH, 2005.
[5] J.W.P. Schmelzer, V.M. Fokin, A.S. Abyzov, E.D. Zanotto, I. Gutzow, Int. J. Appl. Glass Sci. 1 (2010) 16.
[6] T. Hikima, M. Hanaya, M. Oguni, Bull. Chem. Soc. Jpn. 69 (1996) 1863.
[7] T. Hikima, M. Hanaya, M. Oguni, J. Mol. Struct. 479 (1999) 245.
[8] O. Norimaru, M. Oguni, Solid State Commun. 99 (1996) 53.
[9] M. Hatase, M. Hanaya, T. Hikima, M. Oguni, J. Non-Cryst. Solids 307–310 (2003) 257.
[10] F. Paladi, M. Oguni, J. Phys. Condens. Matter 15 (2003) 3909.
[11] F. Paladi, M. Oguni, Phys. Rev. B 65 (2002) 144202.
[12] T. Ichitsubo, E. Matsubara, T. Yamamoto, H.S. Chen, N. Nishiyama, J. Saida, K. Anazawa, Phys. Rev. Lett. 95 (2005) 245501.
[13] T. Ichitsubo, E. Matsubara, H.S. Chen, J. Saida, T. Yamamoto, N. Nishiyama, J. Chem. Phys. 125 (2006) 154502.
[14] T. Ichitsubo, E. Matsubara, J. Saida, H.S. Chen, N. Nishiyama, T. Yamamoto, Adv. Mater. Sci. 18 (2008) 37.
[15] G.P. Johari, M. Goldstein, J. Chem. Phys. 53 (1970) 2372.
[16] K.L. Ngai, J. Non-Cryst. Solids 352 (2006) 404.
[17] S. Capaccioli, K. Kessairi, D. Prevosto, M. Lucchesi, P.A. Rolla, J. Phys. 19 (2006) 205133.
[18] J. Hachenberg, D. Bedorf, K. Samwer, R. Richert, A. Kahl, M.D. Demetriou, W.L. Johnson, Appl. Phys. Lett. 92 (2008) 131911.
[19] M. Goldstein, J. Chem. Phys. 132 (2010) 041104.
[20] The use of Zeldowich's description of induction time (Ya. B. Zeldowich, Sov. Phys. JETP 12 (1942) 525 and Acta Physiochim. USSR 18 (1943) 1) to crystallization of melts and glasses, the readers may consult Ref. [3] here and the discussion in I. Gutzow, D. Kashiev, I. Avramov, J. Non-Cryst. Solids 274 (1985) 208.
[21] E.D. Zanotto, M.L.G. Leite, J. Non-Cryst. Solids 145 (1996) 302.
[22] A. Peker, W.L. Johnson, Appl. Phys. Lett. 63 (1993) 2342.
[23] A. Inoue, Mater. Sci. Forum 179–181 (1995) 691.
[24] W.H. Wang, C. Dong, C.H. Shek, Mater. Sci. Eng. R 44 (2004) 45.
[25] W.H. Wang, Adv. Mater. 21 (2009) 2525.
[26] D.P.B. Aji, P. Wen, G.P. Johari, J. Non-Cryst. Solids 353 (2007) 3796.
[27] D.R. Allen, J.C. Foley, J.H. Perepezko, Acta Mater. 46 (1998) 431.
[28] M.T. Clavaguera-Mora, N. Clavaguera, D. Crespo, T. Pradell, Prog. Mater. Sci. 47 (2002) 559.
[29] G. Shao, Intermetallics 11 (2003) 313.
[30] B.A. Legg, J. Schroers, R. Busch, Acta Mater. 55 (2007) 1109.
[31] L.Q. Xing, J. Eckert, W. Loser, L. Schultz, D.M. Herlach, Philos. Mag. A 79 (1999) 1095.
[32] J.H. Perepezko, R.J. Hebert, R.I. Wu, G. Wilde, J. Non-Cryst. Solids 317 (2003) 52.
[33] K.F. Kelton, T.K. Croat, A.K. Gangopadhyay, L.Q. Xing, A.L. Greer, M. Weyland, X. Li, K. Rajan, J. Non-Cryst. Solids 317 (2003) 71.
[34] B. Van de Moortele, T. Epicier, J.L. Soubeyroux, J.M. Pelletier, Philos. Mag. Lett. 84 (2004) 245.
[35] I. Martin, T. Ohkubo, M. Ohnuma, B. Deconihout, K. Hono, Acta Mater. 52 (2004) 4427.
[36] B.G. Lewis, H.A. Davies, K.D. Ward, in: B. Cantor (Ed.), Proc. 3rd Int. Conf. on Rapidly Quenched Metals, vol. I, The Metal Society, London, 1978, p. 325.
[37] P.H. Shingu, K. Shimomura, R. Ozaki, K. Osamura, Y. Murakami, in: B. Cantor (Ed.), Proc. 3rd Int. Conf. on Rapidly Quenched Metals, vol. I, The Metal Society, London, 1978, p. 315.
[38] C.H. Hwang, K. Cho, K. Kawamura, in: S. Steeb, H. Warlimont (Eds.), Proc. 5th Int. Conf. on Rapidly Quenched Metals, North-Holland, Amsterdam, 1985, p. 331.
[39] A.L. Greer, I.T. Walker, J. Non-Cryst. Solids 317 (2003) 78.
[40] K.F. Kelton, J. Non-Cryst. Solids 163 (1993) 283.
[41] C.V. Thompson, H.J. Frost, F. Spaepen, Acta Metall. 35 (1987) 887.
[42] L.C. Chen, F. Spaepen, J. Appl. Phys. 69 (1991) 679.
[43] A.P. Zhilyaev, G.V. Nurislamova, S. Surinach, M.D. Baro, T.G. Langdon, Mater. Phys. Mech. 5 (2002) 23.
[44] S. Ram, G.P. Johari, Philos. Mag. 61 (1990) 299.
[45] D.P.B. Aji, G.P. Johari, Thermochim. Acta 503–504 (2010) 131.
[46] J.W.P. Schmelzer, J. Non-Cryst. Solids 354 (2008) 269.
[47] G. Adam, J.H. Gibbs, J. Chem. Phys. 43 (1965) 139.
[48] G. Tammann, Die Aggregtazustände (Leopold Voss Verlag, Leipzig,1922); and Der Glaszustand (Leopold Voss Verlag, Leipzig, 1933).
[49] P.W. McMillan, Glass Ceramics, Academic Press, 1964.
[50] J. Hlavac, The Technology of Glass and Ceramics – An Introduction to Glass Science and Technology, vol. 4, Elsevier, New York, 1983.
[51] G.P. Johari, J. Chem. Phys. 58 (1973) 1766.
[52] A. Kahl, T. Koeppe, D. Bedorf, R. Richert, M.L. Lind, M.D. Demetriou, W.L. Johnson, W. Arnold, K. Samwer, Appl. Phys. Lett. 95 (2009) 201903.
[53] G. Power, J.K. Vij, J. Chem. Phys. 120 (2004) 5455.
[54] E. Donth, The Glass Transition: Relaxation Dynamics in Liquids and Disordered Materials, Springer, Berlin, 2001.
[55] K.L. Ngai, M. Paluch, J. Chem. Phys. 120 (2004) 857.
[56] A.N. Kolmogorov, Izv. Acad. Nauk, SSSR, Ser. Mathematica 1 (1937) 355.
[57] W.A. Johnson, R.F. Mehl, Trans. Metall. Soc. AIME 135 (1939) 416.
[58] M. Avrami, J. Chem. Phys. 7 (1939) 1103.
[59] M. Avrami, J. Chem. Phys. 8 (1940) 212.
[60] A.A. Burbelko, E. Fraś, W. Kapturkiewicz, Mater. Sci. Eng. A 429 (2005) 413.
[61] T.J. Bruijn, W.A. De Jong, P.J. Van der Berg, Thermochim. Acta 45 (1981) 315.
[62] A.L. Greer, Acta Metall. 30 (1982) 171.
[63] H. Yinnon, D.R. Uhlmann, J. Non-Cryst. Solids 54 (1983) 253.
[64] H.E. Kissinger, J. Res. NBS 57 (1956) 217.
[65] The reason is that even though the approximations made in the methods used for such analyses are different, KJMA equation is used as a basis in all methods, Yinnon and Uhlmann [63] who showed that, "All these methods are based on the Avrami treatment of transformation kinetics and define an effective crystallization rate coefficient having an Arrhenian temperature dependence." They concluded that [63] "Most are shown to be based on an incorrect neglect of the temperature dependence of the rate coefficient", and "Thus, in general, non-isothermal transformation cannot be treated analytically. A detailed description of non-isothermal transformation can, however, be obtained by numerical methods.".
[66] H. Lu, S. Nutt, J. Appl. Polym. Sci. 89 (2003) 3464.
[67] H.S. Chen, J. Non-Cryst. Solids 27 (1978) 257.
[68] D. Turnbull, B.G. Bagley, Treatise on Solid State Chemistry, vol. 5, Plenum Press, New York, 1975, p. 513.
[69] S.J. Thorpe, B. Ramaswami, K.T. Aust, Acta Metall. 36 (1988) 795.
[70] A.P. Tsai, A. Inoue, Y. Bizen, T. Masumoto, Acta Metall. 37 (1989) 1443.
[71] W.H. Wang, Y.X. Zhuang, M.X. Pan, Y.S. Yao, J. Appl. Phys. 88 (2000) 3914.
[72] D.V. Louzguine, A. Inoue, Appl. Phys. Lett. 78 (2001) 1841.
[73] X. Liu, X. Hui, G. Chen, Mater. Sci. Forum 475–479 (2005) 3385.
[74] Y.T. Shen, L.Q. Xing, K.F. Kelton, Philos. Mag. 85 (2005) 3673.
[75] H.C. Kou, J. Wang, H. Chang, B. Tang, J.S. Li, R. Hu, L. Zhou, J. Non-Cryst. Solids 355 (2009) 420.